Accepted Manuscript

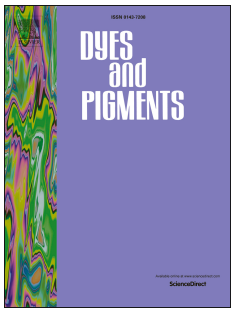

Colorimetric and fluorescence “turn-on” recognition of fluoride by a maleonitrile-based uranyl salen-complex

Silvia Bartocci, Ferran Sabaté, Ramon Bosque, Flore Keymeulen, Kristin Bartik, Laura Rodríguez, Antonella Dalla Cort

PII: S0143-7208(16)30257-1

DOI: 10.1016/j.dyepig.2016.06.006

Reference: DYPI 5290

To appear in: *Dyes and Pigments*

Received Date: 1 March 2016

Revised Date: 31 May 2016

Accepted Date: 4 June 2016

Please cite this article as: Bartocci S, Sabaté F, Bosque R, Keymeulen F, Bartik K, Rodríguez L, Dalla Cort A, Colorimetric and fluorescence “turn-on” recognition of fluoride by a maleonitrile-based uranyl salen-complex, *Dyes and Pigments* (2016), doi: 10.1016/j.dyepig.2016.06.006.

Colorimetric and fluorescence "turn-on" recognition of fluoride by a maleonitrile-based Uranyl Salen-complex

Silvia Bartocci,[1] Ferran Sabaté,[2] Ramon Bosque,[2] Flore Keymeulen,[3] Kristin Bartik,[3] Laura Rodríguez,[2,*] Antonella Dalla Cort.[1,*]

[1] *Dipartimento di Chimica and IMC-CNR Sezione Meccanismi di Reazione, Università La Sapienza, Box 34 Roma 62, 00185 Roma, Italy. Fax: +39 06490421; Tel.: +39 0649913087.*
e-mail address: antonella.dallacort@uniroma1.it

[2] *Departament de Química Inorgànica, Universitat de Barcelona, Martí i Franquès 1-11, 08028 Barcelona, Spain. Fax: +34 934907725; Tel.: +34 934039130.*
e-mail: laura.rodriguez@qi.ub.es

[3] *Engineering of Molecular NanoSystems, Université libre de Bruxelles, 50 avenue F.D. Roosevelt, B-1050 Brussels, Belgium.*

Abstract

The synthesis and characterization of two new uranyl-salen complexes, **1**-**2**, based on a 1,2-diaminomaleonitrile unit, is described. Spectroscopic studies to evaluate their potential as colorimetric probes for fluoride detection in chloroform and dichloromethane were undertaken. Compound **2** exhibits a 'turn-on' response characterized by a naked-eye colorimetric change for the selective recognition of fluoride in both solvents. DFT calculations show that the stabilization energy for the formation of the host:guest complex follows the trend $F^- > Cl^- > Br^-$ hence supporting the experimental data.

Keywords: fluoride recognition; turn-on response; uranyl salen; DFT calculations

1. Introduction

The design of receptors that can selectively recognize a specific analyte amongst a wide range of chemical species is a challenging task in supramolecular chemistry [1,2]. Obtaining a luminescent or colorimetric response, a “naked eye” detection, is furthermore appealing as it enables an easy and straightforward analysis [3]. There is, in particular, an increasing demand for reliable and efficient anion detection as anions play fundamental roles in environmental, industrial, biological, and medical processes [4–6]. In this context fluoride (F^-) is of importance due to its presence in various environmental, clinical and food samples and its controversial toxicity [7,8]. The development of simple and effective fluorescent and/or colorimetric sensors for the fluoride anion is thus the object of reports in the literature [9]. Studies have been undertaken with receptors exploiting different binding paradigms such as boron−fluoride interactions [10], hydrogen bonding with the NH protons of amides [11], indoles [12], pyrroles [13], urea or thiourea [14], Lewis acid coordination [15–17] or anion– π interactions [18]. The visual detection of fluoride has also been obtained by taking advantage of fluoride-promoted cleavage reactions [19]. Although much progress has been made in the area, few easy-to-use systems that operate with high sensitivity have been reported and the development of systems that transform a given binding event into a readable signal remains a challenging task.

While known for a long time, salen/salophen (salen = N,N-ethylenebis(salicylimine), salophen = N,N-phenylenebis(salicylimine)) ligands and the corresponding metal complexes have attracted much attention because they have shown a renewed vitality in the field of catalysis and supramolecular recognition phenomena [20–25]. They can be easily prepared by the reaction of 1,2-ethylendiamine, or 1,2-phenylendiamine, with 2 equivalents of salycilaldehyde. The obtained tetradentate Schiff base ligand coordinates to a variety of transition and main group metals and the properties of the resulting complexes are governed by the coordination geometry of the metal and by the presence of substituents on the ligand skeleton [26–28]. Among the different metals that can be coordinated by these ligands, there is the hexavalent uranyl dication, UO_2^{2+} which has a pentagonal bipyramidal coordination geometry where the apical positions are occupied by the two oxygen atoms of the dication, while four of the five equatorial positions are engaged with the N_2O_2 donor atoms of the ligand [29]. An equatorial position thus remains available for a guest that can be complexed through Lewis acid-base interactions [30]. Uranyl-sal(oph)en complexes have proved to be excellent receptors for fluoride in organic solvents ($K_a > 10^6$ M^{-1}) [17] and such affinity, obviously lowered by the competitive medium, is also preserved when working in water [31–34].

Despite the fact that uranyl ions emit green luminescence, both in the solid state and in solution, and that the sal(oph)en ligand is weakly fluorescencent [35], the combination of the two does not show a significant emission spectrum. Fluoride binding leads only to a very weak change in color of the solution which is not sufficient for an efficient naked-eye detection. In order to develop a selective and visual fluoride sensor which takes advantage of the strong affinity shown by salen-uranyl complexes for fluoride [21], we introduced two cyano substituents on the ligand skeleton [36]. Here we report the synthesis of two new uranyl salen complexes, i.e. uranyl-N,N'-bis(5-tert-butyl-2-hydroxybenzylidene)-1,2-dicyano-1,2-ethenediamine, **1**, and uranyl-N,N'-bis(3,5-ditert-butyl-2-hydroxybenzylidene)-1,2-dicyano-1,2-ethenediamine, **2**, prepared by condensation of 1,2-diaminomaleonitrile with suitable salycilaldehydes in the presence of uranyl acetate (Chart 1). The binding behavior, spectroscopic analysis and theoretical calculations are also described.

Insert Chart 1 here

2. Experimental Section

2.1 Materials

3,5-di-*tert*-butyl-2-hydroxybenzaldehyde, 2,3-diaminomaleonitrile and 4-(*tert*-butyl)phenol were purchased from Aldrich Co. (Milan, Italy). Anhydrous $MgCl_2$ and $UO_2(AcO)_2 \cdot 2H_2O$ were obtained by Fluka Co (Milan, Italy). Paraformaldehyde was obtained by Merck (Milan, Italy). Et_3N and THF were distilled on sodium. Other reagents were of analytical grade and were used without further purification. 5-(tert-butyl)-2-hydroxybenzaldehyde was synthesized following the method described in the literature [37].

2.2 Instruments

^{1}H-NMR and ^{13}C-NMR spectra were recorded on Bruker AC-200 and Bruker AC-300 MHz spectrometers. GC-MS spectra were run on a GC Agilent Technologies 6890N equipped with a 30 m x 0.25 mm x 25 μm methyl silicone gum capillary column containing 5% of phenyl-methyl-silicone (CPSIL8CB) coupled to a 5973MSD Network quadrupole detector operating at 70eV. High-resolution mass spectra (HR-MS) were performed by an ESI-TOF spectrometer. UV-Vis spectra were recorded on Perkin Elmer Lambda 18 and Varian Cary 100 Bio UV-spectrophotometer using spectrophotometric grade $CHCl_3$ and CH_2Cl_2 passed through basic alumina (Al_2O_3) in order to remove acid impurities. The slit width used for UV-Vis emission titrations was 2 nm. Emission spectra were recorded on a Horiba-Jobin-Yvon SPEX Nanolog spectrofluorimeter.

2.3 Computational details

All calculations were carried out with the Gaussian 03 [38] package of programs at the B3LYP computational level [39,40]. The basis set was chosen as follows: for chlorine, bromine and uranium the LANL2DZ basis [41–43] was used. For carbon, hydrogen, fluorine, oxygen and nitrogen the 6-31G(d,p) basis including polarization functions for the non-hydrogen atoms was chosen. Geometries have been optimized in vacuum, without including any symmetry constraints. Solvent effects have been included using the CPCM (polarizable conductor calculation) method on the previously optimized species [44].

2.4 Synthesis

2.4.1 Complex 1. In an one-necked-flask, 5-(*tert*-butyl)-2-hydroxybenzaldehyde, **3** (500 mg, 2.80 mmol), 2,3-diaminomaleonitrile (151 mg, 1.4 mmol) and $UO_2(AcO)_2 \cdot 2H_2O$ (712 mg, 1.68 mmol) were dissolved in the minimum amount of absolute EtOH. The reaction mixture was stirred at 70°C for 48 h. After the precipitation of a dark red solid, the hot solution was filtered collecting 613 mg (0.88 mmol) of product. Yield 73%.

^{1}H-NMR (300 MHz, d_6-DMSO) δ: 9.56 (s, 2H, HC=N), 7.88 (dd, 1H, $^3J_{H\text{-}H}$ = 9 Hz, $^4J_{H\text{-}H}$ = 2.7 Hz), 7.82 (d, 2H, $^4J_{H\text{-}H}$ = 2.7 Hz), 6.95 (d, 1H, $^3J_{H\text{-}H}$ = 8.7 Hz), 1.29 (s, 18H, $C(CH_3)$).

^{13}C-NMR (75 MHz, d_6-DMSO) δ: 170.4, 170.0, 141.0, 137.9, 132.9, 122.6, 121.7, 121.5, 113.7, 34.1, 31.8, 31.5, 31.4.

FT-IR (KBr film) ῡ: 3410, 2959, 2220 (CN-). 1600, 1530, 1463, 1388, 1300, 1255, 1167, 1031, 970, 909, 835, 758, 678, 626, 521, 433

MS-ESI-TOF for $C_{26}H_{26}N_4O_4U$ calcd 696.25, found 697.2522 $[M + H]^+$

Elemental analysis for $C_{26}H_{26}N_4O_4U \cdot EtOH$ calcd: C 45.29%, H 4.34%, N 7.54%, found C 45.15%, H 4.44%, N 7.40%.

2.4.2 Complex 2. In an one-necked-flask, 3,5-di-*tert*-butyl-2-hydroxybenzaldehyde (469 mg, 2 mmol), 2,3-diaminomaleonitrile (108 mg, 1 mmol) and $(AcO)_2UO_2 \cdot 2H_2O$ (509 mg, 1.2 mmol) were dissolved in the minimum amount of absolute EtOH. The reaction mixture was stirred at 70°C for 48 h. After the precipitation of a dark violet solid, the hot solution was filtered collecting 485 mg (0.60 mmol). Yield 60%.

^{1}H-NMR (200 MHz, $CDCl_3$) δ: 9.56 (s, 2H, HC=N), 7.93 (d, 2H, Ph, $^4J_{H\text{-}H}$ = 2 Hz), 7.47 (d, 2H, Ph, $^4J_{H\text{-}H}$ = 2 Hz), 1.49 (s, 18H, $C(CH_3)_3$), 1.21 (s, 18H, $C(CH_3)_3$).

^{13}C-NMR (25 MHz, $CDCl_3$) δ: 171.1, 169.5, 141.2, 140.5, 135.5, 131.2, 124.2, 112.7, 35.1, 34.0, 31.2, 29.7.

FT-IR (KBr film) ῡ: 3560, 2955, 2223 (CN-), 1570, 1533, 1420, 1296, 1257, 1173, 1043, 973.908.

M**S-ESI-TOF** for $C_{34}H_{42}N_4O_4NaU$ calcd 831.3766, found 831.3755 m/z^+.

Elemental analysis for $C_{34}H_{42}N_4O_4U \cdot H_2O$ calcd: C 49.39%, H 5.36%, N 6.78%, found C 48.94%, H 5.85%, N 6.53%.

2.5 UV-Vis titrations

UV-Vis titrations for uranyl salophens were carried out at 25 ºC in air-equilibrated chloroform or dichloromethane (spectrophotometric grade). The initial receptor concentration is chosen in order to

have its spectrum absorbance comprised between 0 and 1 and the expected association constant value determines the concentration range of the guest collecting as many points as possible in the non-linear part of the binding hyperbola (equation 1).

$$A = A_0 + \Delta A_\infty \frac{[R_0] + 1/K + [G] - [([R_0] + 1/K + [G])^2 - 4[G][R_0]]^{1/2}}{2[R_0]} \quad \text{Eq. 1}$$

A = experimental absorbance

A_0 = initial absorbance of the receptor

$[R_0]$ = analytical concentrantion of the receptor

[G] = total guest concentration in each point, including that fraction bound to the receptor.

3. Results and Discussion

3.1 Synthesis and Characterization

Complexes **1** and **2** were synthesized according to **Scheme 1**.

Please, insert here Scheme 1

The 5-(*tert*-butyl)-2-hydroxybenzaldehyde was synthesized through regioselective formylation of 4-*tert*-butylphenol, mediated by $MgCl_2$ acting as chelating intermediate [37]. The condensation reaction between this aldehyde and the 1,2-dicyano 1,2-diamine in the presence of uranyl acetate [45] leads to the formation of the complexes whose characterization, performed by different spectroscopic techniques together with mass spectrometry, confirmed their successful formation. ^{1}H-NMR showed the presence of the imine protons and ^{13}C-NMR the typical salen resonances (Figures S1 and S2, SI). IR spectra (Figures S4 and S7, SI) display the typical band ($\tilde{\upsilon}$(C≡N) ~ 2222 cm^{-1}) of the cyano group and the molecular peaks were observed in both cases by mass spectrometry.

3.2 Halide recognition studies

Spectroscopic studies were carried out in order to investigate the binding properties of the two compounds. Chloroform and dichloromethane were used as a non-coordinating solvent to avoid competition with the guest for the binding site of the complex. Molecular recognition processes were followed mainly by UV-Vis absorption titrations using the tetrabutylamonium salts of fluoride (TBAF), chloride (TBACl) and bromide (TBABr).

Absorption spectra of the uranyl complexes display two main bands at *ca*. 480 and 580 nm which can be assigned to π–π^* transitions [30]. The addition of fluoride, chloride and bromide to the chloroform solution of receptor **1** induces a similar color change in all cases, Fig 1.

Please, insert here Figure 1

It is known that in non-coordinating solvents uranyl-salophen complexes without bulky substituents in the 3,3'-positions, the ones *ortho* to the phenolic oxygen, are present as dimeric complexes $[(UO_2(salophen)]_2$ even at low concentrations (10^{-5}-10^{-6} M) [46]. The same behavior can be

predicted for salen derivatives [47] and indeed the broad peaks in the ^{1}H NMR spectrum of **1** in $CDCl_3$ confirm this (Figure S3, SI). It was thus not possible to undertake quantitative studies of the binding affinity of complex **1** toward halides: the strong affinity of halides for the metal center leads, upon salt addition, to the dissociation of the dimer due to the formation of the host-guest complex and this additional equilibrium complicates the analysis of the data. The addition of increasing amounts of TBAF to the chloroform solution of **1** leads to a 30% increase of the intensity of the lowest energy absorption band. This is not observed with chloride and bromide (see SI, Figures S11, S12, S13).

The higher solubility of **1** in CH_2Cl_2 allowed the preparation of solutions of known concentration to perform quantitative investigations. The binding affinities of **1**, reported in Table 1, were determined via UV-vis titration experiments using the different halide salts and considering a 1:1 coordination model (verified by a Job Plot, Figure 2 right). As expected, the trend in binding affinities is in agreement with anion hardness: F^-> Cl^-> Br^-. We observed that the lowest energy absorption band shows, upon complete saturation of the binding site, a 2-fold increase in intensity in the presence of F^-, while only a 25% and 15% increase is observed for Cl^- and Br^- respectively (see SI, Figures S8, S9, S10).

Please, insert here Table 1

To prevent the formation of dimers and increase the solubility of the salen derivatives in chloroform, we synthesized complex **2** through the condensation of commercially available 3,5-di-*tert*-butyl-2-hydroxybenzaldehyde with 2,3-diaminonitrile in the presence of $UO_2(AcO)_2 \cdot 2H_2O$, in ethanol (Scheme S2, SI). This time the ^1H NMR spectrum in $CDCl_3$ showed well-resolved sharp peaks confirming the absence of dimers (Figure S5, SI) whose formation is prevented by the presence of the bulky *tert*-butyl groups (see theoretical studies described below). The affinity of **2** for fluoride, chloride and bromide in chloroform were determined, via UV-Vis absorption titration experiments (Figure 2) and are reported in Table 1. The presence of sharp isosbestic points at 495 and 560 nm confirms the 1:1 association.

Please, insert here Figure 2

Remarkably, in chloroform the addition of fluoride and chloride to the solution of **2** causes a change of color that is not observed with bromide, Figure 3. The solution to which fluoride is added turns to a greenish tinge, while with chloride it becomes light blue. Red shifts are observed for the lowest energy absorption band upon titration (*ca*. 25 nm for F^- and 10 nm for Cl^-)

Please, insert here Figure 3

Titrations were also undertaken in dichloromethane and the affinity constants derived from these experiments are reported in Table 1. We tried to investigate the luminescent properties of these compounds in both solvents. As mentioned in the introduction, generally, uranyl-salophen/salen complexes are not luminescent at ambient conditions. The uranyl ion UO_2^{2+} is characterized by a low energy oxide to uranium(VI) ligand-to-metal charge transfer (LMCT) state which is emissive under ambient conditions. However, a large variety of ligands, i.e. halides, carboxylates, N,N-bis(salicylidene)-1,2-ethylene diamine derivatives etc., when coordinated as additional ligands in the plane perpendicular to the O=U=O axis cause luminescence quenching [48].

The absence of any luminescence of UO_2(sal(oph)en) can then be only explained by the presence of lower energy salophen^{2-} to U(VI) LMCT states which are rapidly populated from the IL states. These LMCT states are apparently not emissive [48]. No emission spectrum is observed for **1** and **2** in chloroform and in dichloromethane but when adding fluoride to complex **2** in chloroform an emission band at 478 nm is observed (Figure 4). This is not the case with the other halides and it

does not happen in dichloromethane where the change of color is also observed. Hence, **2** can be considered as a fluorescence "turn-on" probe for fluoride detection. It was unfortunately not possible to measure the binding constant through emission titrations because, even after the addition of a very large excess of TBAF, greater than 10 equivalents, fluorescence emission did not reach the saturation thus preventing ratiometric detection. As far as we know, there are very few reports where fluoride binding is associated with a fuorescence 'turn-on' response along with a colorimetric change detectable by the naked eye [49,50]. Complex **2** is therefore a promising candidate to behave as a selective receptor for fluoride in $CHCl_3$, and also in CH_2Cl_2 using UV-Vis and fluorescence spectroscopies and as colorimetric sensor through "naked eye" recognition thanks to the selective color change of the solutions.

Please, insert here Figure 4

We undertook preliminary experiments in a more competitive solvent, methanol, and, as expected, the binding constant between receptor **2** and fluoride drops at least three orders of magnitude (SI).

3.3 DFT theoretical studies

3.3.1 Molecular modeling

In order to rationalize the experimental results we have performed some theoretical calculations at the DFT level, using the B3LYP functional [39,40]. Molecular modeling was performed in order to analyze in more detail the expected geometry of the complexes. The minimum energy geometries of **1** and **2** are displayed in Figure 6 and show that, in principle, no steric hindrance preclude guest molecule hosting in the fifth equatorial binding site of the metal.

Please, insert here Figure 5

The main calculated distances are shown in Table 2 and are found to be perfectly in agreement with those retrieved from x-ray crystal structure data of uranyl salen complexes previously reported in the literature [51].

Please, insert here Table 2

The U–O distance, is significantly longer than the axial oxygens (U=O) due to the overlap between the 6d and 5f orbitals of the uranium atom and the three p orbitals (or two p and one hybrid sp orbitals) of each axial oxygen giving the linear structure [52]. U-N distances are typically found to be longer than U–O distances, indicating that the coordination of the oxygen atom is stronger than that of the nitrogen atom. Furthermore, the larger U–N value can also be explained in terms of Pearson's hard and soft acid–base concept [51]. These U-O and U-N distances are predicted to be slightly longer for complex **1** with only one *tert*-butyl substituent in the salophen aromatic ligand.

To obtain an insight into the formation of dimers, we carried out calculations for both receptors. Indeed the most stable conformation for dimer formation is obtained in the case of compound **1**, which does not have substituents at 3,3' positions (Figure 6, left) so confirming that steric bulkiness in these positions prevents the formation of dimeric species.

Please, insert here Figure 6

3.3.2 Absorption data

Density functional studies were used to verify the host and guest complexation from a theoretical perspective. They were performed in order to rationalize the experimental UV-visible spectra of the complexes and verify the assignment of the observed transition bands. Chloroform solvent was chosen as a model. Three main absorption bands have been calculated to be at 559, 498, 392 and 371 nm, for **1**, and 560, 519 and 410 nm and, for **2**, respectively, in agreement with the experimental bands located at 579, 480 and 388 nm (complex **1**) and 586, 503 and 395 nm (for complex **2**). These bands can be assigned to HOMO-2 → LUMO+1, HOMO-2 → LUMO+3 and HOMO → LUMO+5, (complex **1**) and HOMO → LUMO+3, HOMO-2 → LUMO+1 and HOMO-2 → LUMO+3 (complex **2**) transitions. Inspection of Figures 7 and S20 lead us to verify that the electronic density of the orbitals are mainly located at the aromatic salen group in agreement with the previously assigned π–π* transition.

Please, insert here Figure 7

3.3.3 Stability of the host:guest adducts

The energies for the formation of the uranyl complexes: halide adducts were calculated by DFT in the gas phase and in the two different solvents used in the experimental titrations (dichloromethane and chloroform) and the results are summarized in Table 3.

Please, insert here Table 3

Inspection of Table 3 confirms the experimental picture. The affinity for fluoride anion is the highest for both receptors, in all conditions, following the general trend being $F^- > Cl^- > Br^-$. The recognition process seems also to be more efficient in chloroform in good agreement with the data reported in Table 1. On the other hand, the energies predicted for the host:guest interactions with **2** are larger than those calculated for the same processes with **1**. These data are coherent with the experimental ones and point out the more efficient binding process taking place when the two *tert*-butyl substituents are present. We calculated also the distances between the metal center and the bound anion, U···X(X = F^-, Cl^-, Br^-), and these are 2.133, 2.718 and 2.931 Å respectively for complex **2** (Figure 8). They reproduce quite nicely those obtained from X-ray crystal diffraction in analogous host-guest uranyl-halide complexes [53,54]. Similar values could be expected for adducts with complex **1**, being the U···X distances 2.111, 2.707 and 2.921 for X = F^-, Cl^-, Br^- respectively (see Figure S21).

Please, insert here Figure 8

4. Conclusions

In conclusion, we report here on two newly synthesized maleonitrile-based uranyl-salen derivatives, **1**-**2**, and their use as potential colorimetric probes for halide detection in organic solvents, i.e. chloroform and dichloromethane. The low solubility of compound **1**, prevented the quantitative measurements of its binding affinity toward anions in $CHCl_3$, but not in CH_2Cl_2. The selectivity trend $F^->Cl^->Br^-$ is in agreement with anion hardness. A non-selective change of the color of the dichloromethane solution occurred upon addition of fluoride, chloride and bromide. The addition of fluoride and chloride to the solution of **2** in $CHCl_3$, and also in CH_2Cl_2, caused a change of color that is not observed in the case of bromide. Moreover, only the presence of F^- induces the appearance of an emission band centered at 478 nm in an otherwise "flat" emission spectrum of **2**. Thus receptor **2** can be regarded as a fluorescence "turn-on" probe for fluoride detection, and also as a chromogenic probe. As far as we know, there are very few reports in the literature about fluoride ion binding associated with a fluorescence 'turn-on' response along with a colorimetric change detectable by the naked eye. DFT calculations provided theoretical support to the host and guest investigation. Host:guest adduct stabilities were calculated in vacuum, dichloromethane and chloroform and the results are in agreement with the experimental data. On the other hand, the higher stability of the dimer formation in the case of **1**, justifies the higher difficulty on the molecular recognition process.

Acknowledgments

The support and sponsorship provided by COST Action CM1005 is acknowledged. Authors are also grateful to the Ministerio de Ciencia e Innovación of Spain (Project CTQ2015-65040-P). A.D.C. aknowledges "Ricerca scientifica di Ateneo 2014" and MIUR "PRIN 2010CX2TLM". F.K thanks the FNRS for her PhD Grant.

Supporting Information

^{1}H-NMR spectrum (300 MHz – DMSO-d_6) of complex **1** (Figure S1); ^{13}C-NMR spectrum (75 MHz – DMSO-d_6) of complex **1** (Figure S2); ^{1}H-NMR spectrum of **1** in $CDCl_3$ (Figure S3); FT-IR spectrum (KBr film) of complex **1** (Figure S4); ^{1}H-NMR spectrum (200 MHz – $CDCl_3$) of complex **2** (Figure S5); ^{13}C-NMR spectrum (25 MHz – $CDCl_3$) of complex **2** (Figure S6); FT-IR spectrum (KBr film) of complex **1** (Figure S7); UV-Vis spectrum of complex **1** ($5\cdot10^{-5}$M) with increasing amount of F^- in CH_2Cl_2 (Figure S8); UV-Vis spectrum of complex **1** ($5\cdot10^{-5}$M) with increasing amount of Cl^- in CH_2Cl_2 (Figure S9); UV-Vis spectrum of complex **1** ($5\cdot10^{-5}$M) with increasing amount of Br^- in CH_2Cl_2 (Figure S10); UV-Vis spectrum of complex **1** ($5\cdot10^{-5}$M) with increasing amount of F^- in $CHCl_3$ (Figure S11); UV-Vis spectrum of complex **1** ($5\cdot10^{-5}$M) with increasing amount of Cl^- in $CHCl_3$ (Figure S12); UV-Vis spectrum of complex **1** ($5\cdot10^{-5}$M) with increasing amount of Br^- in $CHCl_3$ (Figure S13); UV-Vis spectrum of complex **2** ($5\cdot10^{-5}$M) with increasing amount of F^- in CH_2Cl_2 (Figure S14); UV-Vis spectrum of complex **2** ($5\cdot10^{-5}$M) with increasing amount of Cl^- in CH_2Cl_2 (Figure S15); UV-Vis spectrum of complex **2** ($5\cdot10^{-5}$M) with increasing amount of Br^- in CH_2Cl_2 (Figure S16); UV-Vis spectrum of complex **2** ($5\cdot10^{-5}$M) with increasing amount of F^- in $CHCl_3$ (Figure S17); UV-Vis spectrum of complex **2** ($5\cdot10^{-5}$M) with increasing amount of Cl^- in $CHCl_3$ (Figure S18); UV-Vis spectrum of complex **2** ($5\cdot10^{-5}$M) with increasing amount of Br^- in $CHCl_3$ (Figure S19); UV-Vis spectrum of complex **2** ($5\cdot10^{-5}$M) with increasing amount of F^- in methanol (Figure S20); UV-Vis spectrum of complex **2** ($5\cdot10^{-5}$M) with increasing amount of Cl^- in methanol (Figure S21); UV-Vis spectrum of complex **2** ($5\cdot10^{-5}$M) with increasing amount of Br^- in methanol (Figure S22); HOMO and LUMO orbital transition of complex **1** (Figure S23); Molecular modeling of complex **1** with F^-, Cl^- and Br^- (Figure S24).

References

[1] Anslyn E V. Supramolecular Analytical Chemistry Supramolecular Analytical Chemistry. J Org Chem 2007;72:687–99. doi:10.1021/jo0617971.

[2] Pinalli R, Dalcanale E. Supramolecular sensing with phosphonate cavitands. Acc Chem Res 2013;46:399–411. doi:10.1021/ar300178m.

[3] Wu J, Kwon B, Liu W, Anslyn E V, Wang P, Kim JS. Chromogenic/Fluorogenic Ensemble Chemosensing Systems. Chem Rev 2015;115:7893–943. doi:10.1021/cr500553d.

[4] Das A, Ghosh S. Stimuli-Responsive Self-Assembly of a Naphthalene Diimide by Orthogonal Hydrogen Bonding and Its Coassembly with a Pyrene Derivative by a Pseudo-Intramolecular Charge-Transfer Interaction. Angew Chemie Int Ed 2014;53:1092–7. doi:10.1002/anie.201308396.

[5] Kubik S. Amino acid containing anion receptors. Chem Soc Rev 2009;38:585–605. doi:10.1039/b810531f.

[6] Gale PA, Caltagirone C. Anion sensing by small molecules and molecular ensembles. Chem Soc Rev 2014;44:4212–27. doi:10.1039/c4cs00179f.

[7] Cametti M, Rissanen K. Recognition and sensing of fluoride anion. Chem Commun 2009:2809–29. doi:10.1039/b902069a.

[8] Tressaud A, Haufe G. Fluorine and Health, Molecular Imaging, Biomedical Materials and Pharmaceuticals. 2012. doi:10.1016/B978-0-444-53086-8.00001-1.

[9] Zhou Y, Zhang JF, Yoon J. Fluorescence and colorimetric chemosensors for fluoride-ion detection. Chem Rev 2014;114:5511–71. doi:10.1021/cr400352m.

[10] Zhao H, Leamer LA, Gabbaï FP. Anion capture and sensing with cationic boranes: on the synergy of Coulombic effects and onium ion-centred Lewis acidity. Dalton Trans 2013;42:8164–78. doi:10.1039/c3dt50491c.

[11] Qu Y, Hua J, Tian H. Colorimetric and Ratiometric Red Fluorescent Chemosensors for Fluoride Ion Based on Diketopyrrolopyrrole. Org Lett 2010;12:3320–3. doi:10-1021/ol101081m.

[12] Caltagirone C, Gale PA, Hiscock JR, Hursthouse MB, Light ME, Tizzard GJ. 2-Amidoindole-based anion receptors. Supramol Chem 2009;21:125–30. doi:10.1080/10610270802348243.

[13] Kim DS, Sessler JL. Calix[4]pyrroles: versatile molecular containers with ion transport, recognition, and molecular switching functions. Chem Soc Rev 2015;44:532–46. doi:10.1039/c4cs00157e.

[14] Li A-F, Wang J-H, Wang F, Jiang Y-B. Anion Complexation and sensing using modified

urea and thiourea-based receptors. Chem Soc Rev 2010;39:3729–45. doi:10.1039/b926160p.

[15] Jeremies A, Lehmann U, Gruschinski S, Schleife F, Meyer M, Matulis V, et al. Cavitands Incorporating a Lewis Acid Dinickel Chelate Function as Receptors for Halide Anions. Inorg Chem 2015;54:3937–50. doi:10.1021/acs.inorgchem.5b00123.

[16] Goursaud M, De Bernardin P, Dalla Cort A, Bartik K, Bruylants G. Monitoring fluoride binding in DMSO: Why is a singular binding behavior observed? European J Org Chem 2012:3570–4. doi:10.1002/ejoc.201200165.

[17] Cametti M, Dalla Cort A, Mandolini L, Nissinen M, Rissanen K. Specific recognition of fluoride anion using a metallamacrocycle incorporating a uranyl-salen unit. New J Chem 2008;32:1113. doi:10.1039/b806149a.

[18] Frontera A, Gamez P, Mascal M, Mooibroek TJ, Reedijk J. Putting anion-π interactions into perspective. Angew Chemie - Int Ed 2011;50:9564–83. doi:10.1002/anie.201100208.

[19] Gai L, Mack J, Lu H, Nyokong T, Li Z, Kobayashi N, et al. Organosilicon compounds as fluorescent chemosensors for fluoride anion recognition. Coord Chem Rev 2015;285:24–51. doi:10.1016/j.ccr.2014.10.009.

[20] Whiteoak CJ, Salassa G, Kleij AW. Recent advances with π-conjugated salen systems. Chem Soc Rev 2012;41:622. doi:10.1039/c1cs15170c.

[21] Jacobsen EN. Asymmetric catalysis of epoxide ring-opening reactions. Acc Chem Res 2000;33:421–31. doi:10.1021/ar960061v.

[22] Dalla Cort A, De Bernardin P, Forte G, Mihan FY. Metal–salophen-based receptors for anions. Chem Soc Rev 2010;39:3863–74. doi:10.1039/b926222a.

[23] Clarke RM, Storr T. The chemistry and applications of multimetallic salen complexes. Dalton Trans 2014;43:9380–91. doi:10.1039/c4dt00591k.

[24] Yafteh Mihan F, Bartocci S, Bruschini M, De Bernardin P, Forte G, Giannicchi I, et al. Ion-Pair Recognition by Metal - Salophen and Metal - Salen Complexes. Aust J Chem 2012;65:1638–46. doi:10.1071/CH12353.

[25] Cano M, Rodriguez L, Lima JC, Pina F, Dalla Cort A, Pasquini C, et al. Specific supramolecular interactions between Zn2+-salophen complexes and biologically relevant anions. Inorg Chem 2009;48:6229–35. doi:10.1021/ic900557n.

[26] Brissos R, Ramos D, Lima JC, Yafteh Mihan F, Borras M, de Lapuente J, et al. Luminescent Zinc salophen derivatives: cytoxicity assessment and action mechanism studies. New J Chem 2013:1046–55. doi:10.1039/c3nj41125g.

[27] Giannicchi I, Brissos R, Ramos D, Lapuente J De, Lima C, Dalla Cort A, et al. Substituent E ff ects on the Biological Properties of Zn-Salophen Complexes. Inorg Chem 2013;52:9245–

53.

[28] Cametti M, Dalla Cort A, Mandolini L. Substituent effects in cation–π interactions. Recognition of tetramethylammonium chloride by uranyl-salophen receptors. Chem Sci 2012;3:2119. doi:10.1039/c2sc00675h.

[29] Sessler J, Melfi P, Pantos G. Uranium complexes of multidentate N-donor ligands. Coord Chem Rev 2006;250:816–43. doi:10.1016/j.ccr.2005.10.007.

[30] van Axel Castelli V, Dalla Cort A, Mandolini L, Pinto V, Reinhoudt DN, Ribaudo F, et al. Molecular Recognition of Carbonyl Compounds by Uranyl-salophen Based Neutral Receptors Driven by Van Der Waals Forces. Supramol Chem 2002;14:211–9. doi:10.1080/10610270290026112.

[31] Dalla Cort A, Forte G, Schiaffino L. Anion recognition in water with use of a neutral uranyl-salophen receptor. J Org Chem 2011;76:7569–72. doi:10.1021/jo201213e.

[32] Bedini E, Forte G, De Castro C, Parrilli M, Dalla Cort A. A route to oligosaccharide-appended salicylaldehydes: Useful building blocks for the synthesis of metal-salophen complexes. J Org Chem 2013;78:7962–9. doi:10.1021/jo401148f.

[33] Cametti M, Dalla Cort A, Bartik K. Fluoride binding in water: A new environment for a known receptor. ChemPhysChem 2008;9:2168–71. doi:10.1002/cphc.200800412.

[34] Keymeulen F, De Bernardin P, Giannicchi I, Galantini L, Bartik K, Dalla Cort A. Fluoride binding in water with the use of micellar nanodevices based on salophen complexes. Org Biomol Chem 2015;13:2437–43. doi:10.1039/c4ob02298j.

[35] Liu K, Huo J, Zhu B, Huo R. Fluoride-triggered ESPT in the binding with sal(oph)en. J Fluoresc 2012;22:1231–6. doi:10.1007/s10895-012-1063-z.

[36] Hardwick HC, Royal DS, Helliwell M, Pope SJA, Ashton L, Goodacre R, et al. Structural, spectroscopic and redox properties of uranyl complexes with a maleonitrile containing ligand. Dalt Trans 2011;40:5939. doi:10.1039/c0dt01580f.

[37] Verner E, Katz B a, Spencer JR, Allen D, Hataye J, Hruzewicz W, et al. Development of serine protease inhibitors displaying a multicentered short (<2.3 A) hydrogen bond binding mode: inhibitors of urokinase-type plasminogen activator and factor Xa. J Med Chem 2001;44:2753–71.

[38] Frisch MJ, Trucks GW, Schlegel HB, Scuseria GE, Robb MA, Cheeseman JR, Montgomery Jr JA, Vreven T, Kudin KN, Burant JC, Millan JM, Iyengar SS, Tomasi J, Barone V, Mennucci B, Cossi M, Scalmani G, Rega N, Petersson GA, Nakatsuji H, Hada M, Ehara M, Toyota K, Fukuda R, Hasegawa J, Ishida M, Nakajima T, Honda Y, Kitao O, Nakai H, Klene M, Li X, Knox JE, Hratchian HP, Cross JB, Bakken V, Adamo C, Jaramillo J, Gomperts R,

Stratmann RE, Yazyev O, Austin AJ, Cammi R, Pomelli C, Ochterski JW, Ayala PY, Morokuma K, Voth GA, Salvador P, Dannenberg JJ, Zakrzewski VG, Dapprich S, Daniels AD, Strain MC, Farkas O, Malick DK, Rabuck AD, Raghavachari K, Foresman JB, Ortiz JV, Cui Q, Baboul AG, Clifford S, Cioslowski J, Stefanov BB, Liu G, Liashenko A, Piskorz P, Komaromi I, Martin RL, Fox DJ, Keith T, Al-Laham MA, Peng CY, Nanayakkara A, Challacombe M, Gill PMW, Johnson B, Chen W, Wong MW, Gonzalez C, Pople JA. Gaussian 03, Revision C.02. Gaussian, Inc., Wallingford CT 2004.

[39] Becke AD. Density-functional thermochemistry.III. The role of exact exchange. J Chem Phys 1993;98:5648. doi:10.1063/1.464913.

[40] Lee C, Yang W, Parr RG. Development of the Colle-Salvetti correlation-energy formula into a functional of the electron density. Phys Rev B 1988;37:785–9. doi:10.1103/PhysRevB.37.785.

[41] Wadt WR, Hay PJ. Ab initio effective core potentials for molecular calculations. Potentials for main group elements Na to Bi. J Chem Phys 1985;82:284–98. doi:10.1063/1.448800.

[42] Wadt WR, Hay PJ. Ab initio effective core potentials for molecular calculations. Potentials for K to Au including the outermost core orbitarls. J Chem Phys 1985;82:299–301. doi:10.1063/1.448975.

[43] Otriz, J, Hay P, Martin R. Role of d and f orbitals in the geometries of low-valent actinide compounds. Ab initio studies of U(CH3)3, Np(CH3)3, and Pu(CH3)3. J Am Chem Soc 1992;114:2736–7. doi:10.1021/ja00033a068.

[44] Cossi M, Rega N, Scalmani G, Barone V. Energies, structures, and electronic properties of molecules in solution with the C-PCM solvation model. J Comput Chem 2003;24:669–81. doi:10.1002/jcc.10189.

[45] Lacroix PG, Di Bella S, Ledoux I. Synthesis and Second-Order Nonlinear Optical Properties of New Copper(II), Nickel(II), and Zinc(II) Schiff-Base Complexes. Toward a Role of Inorganic Chromophores for Second Harmonic Generation. Chem Mater 1996;8:541–5. doi:10.1021/cm950426q.

[46] Koichiro Takao YI. Structural Characterization and Reactivity of UO2 (salophen)L and [UO2(salophen)]2 : Dimerization of UO2(salophen) Fragments in Noncoordinating Solvents (salophen). Inorg Chem 2007;46:4–7.

[47] Consiglio G, Failla S, Finocchiaro P, Oliveri I Pietro, Di Bella S. An unprecedented structural interconversion in solution of aggregate zinc(II) salen Schiff-base complexes. Inorg Chem 2012;51:8409–18. doi:10.1021/ic300954y.

[48] Kunkely H, Vogler A. Excited State Behavior of Uranyl Complexes with Salophen and

Oxine as Chromophoric Ligands. Z Naturforsch 2002;57b:301–4.

[49] Peng Y, Dong YM, Dong M, Wang YW. A selective, sensitive, colorimetric, and fluorescence probe for relay recognition of fluoride and Cu(II) ions with “off-On-Off” switching in ethanol-water solution. J Org Chem 2012;77:9072–80. doi:10.1021/jo301548v.

[50] Balamurugan A, Lee H I L. Single molecular probe for multiple analyte sensing: Efficient and selective detection of mercury and fluoride ions. Sensors Actuators, B Chem 2015;216:80–5. doi:10.1016/j.snb.2015.04.026.

[51] Azam M, Al-Resayes SI, Velmurugan G, Venuvanalingam P, Wagler J, Kroke E. Novel uranyl(VI) complexes incorporating propylene-bridged salen-type N2O2-ligands: a structural and computational approach. Dalton Trans 2015;44:568–77. doi:10.1039/c4dt02112f.

[52] Venkateswara Rao P, Rao CP, Sreedhara A, Wegelius EK, Rissanen K, Kolehmainen E. Synthesis, structure and reactivity of trans-UO22+ complexes of OH-containing ligands. J Chem Soc Dalton Trans 2000;56:1213–8. doi:10.1039/b000142m.

[53] Cametti M, Nissinen M, Dalla Cort A, Mandolini L, Rissanen K. Uranyl-salophen based ditopic receptors for the recognition of quaternary ammonium halides. Chem Commun 2003:2420–1. doi**:** 10.1039/B307849C.

[54] Cametti M, Nissinen M, Dalla Cort A, Mandolini L, Rissanen K. Ion pair recognition of quaternary ammonium and iminium salts by uranyl-salophen compounds in solution and in the solid state. J Am Chem Soc 2007;129:3641–8. doi:10.1021/ja068561z.

Figures

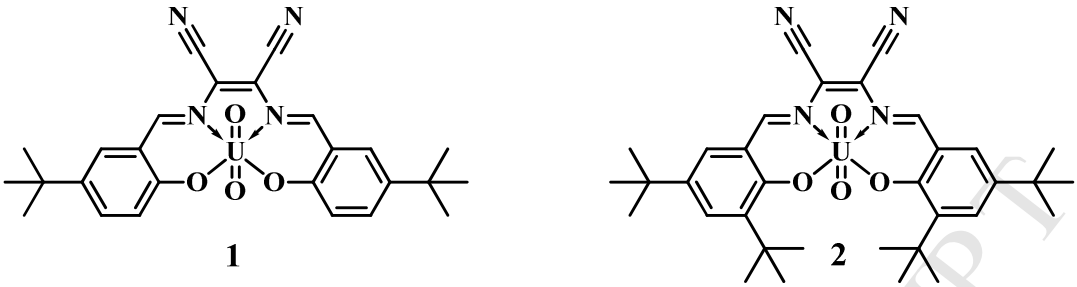

Chart 1

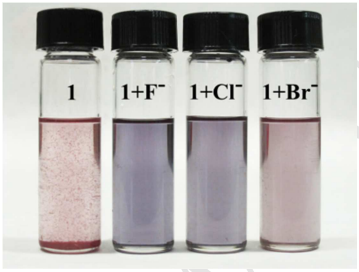

Figure 1

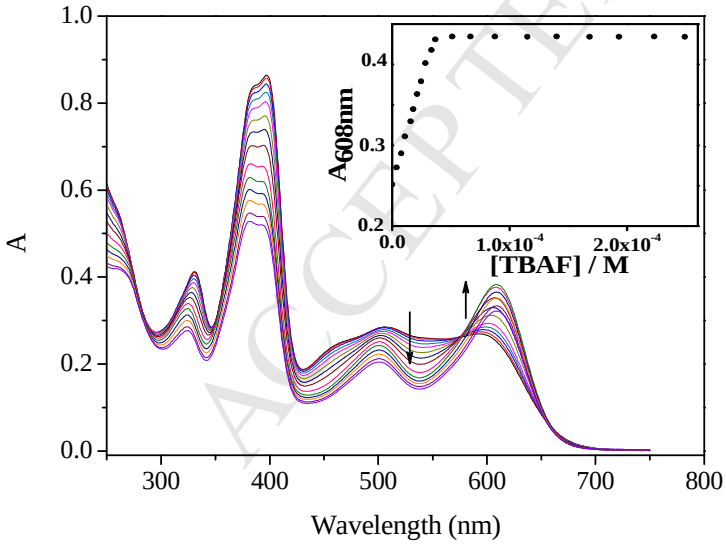

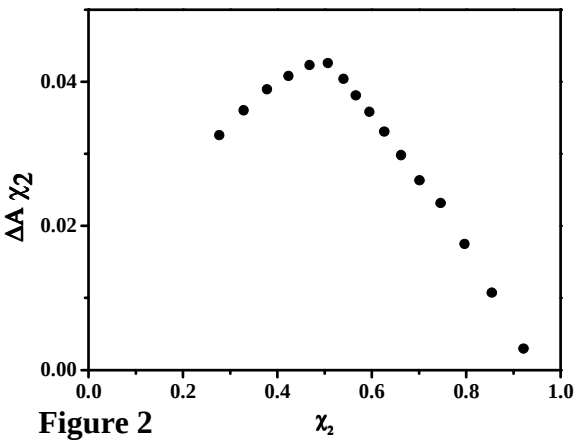

Figure 2

Figure 3

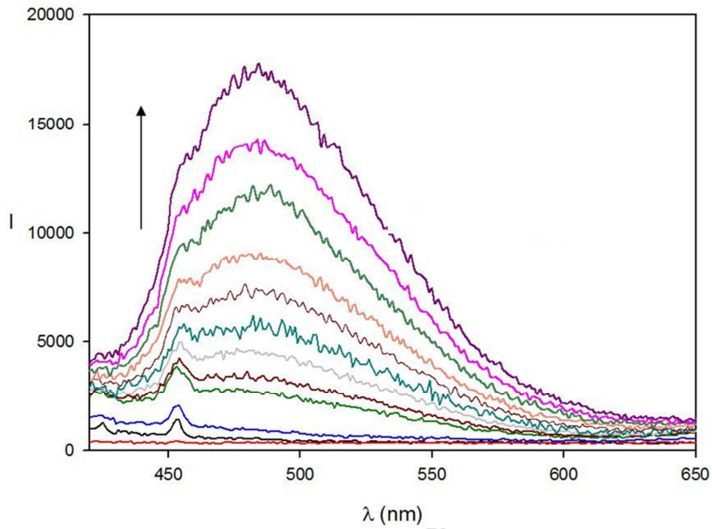

Figure 4

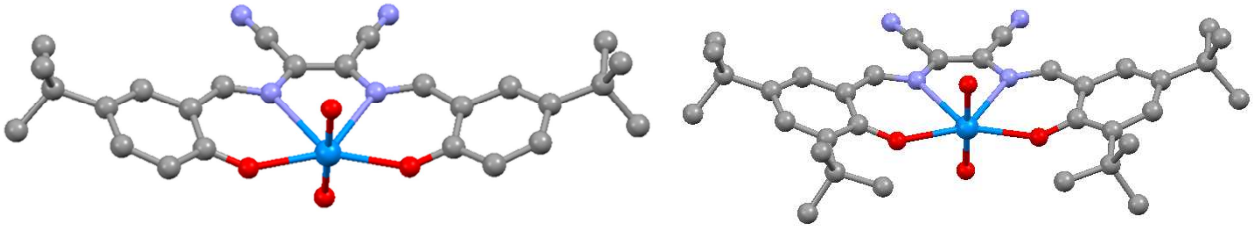

Figure 5

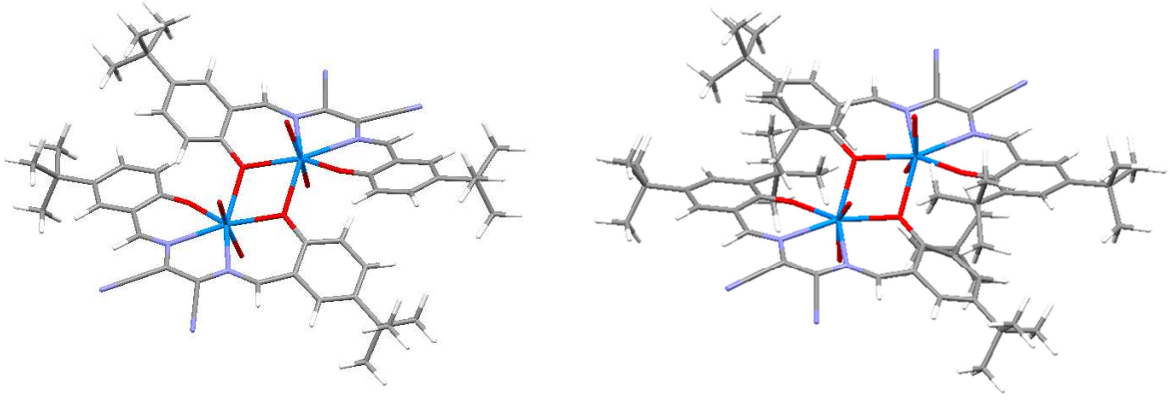

Figure 6

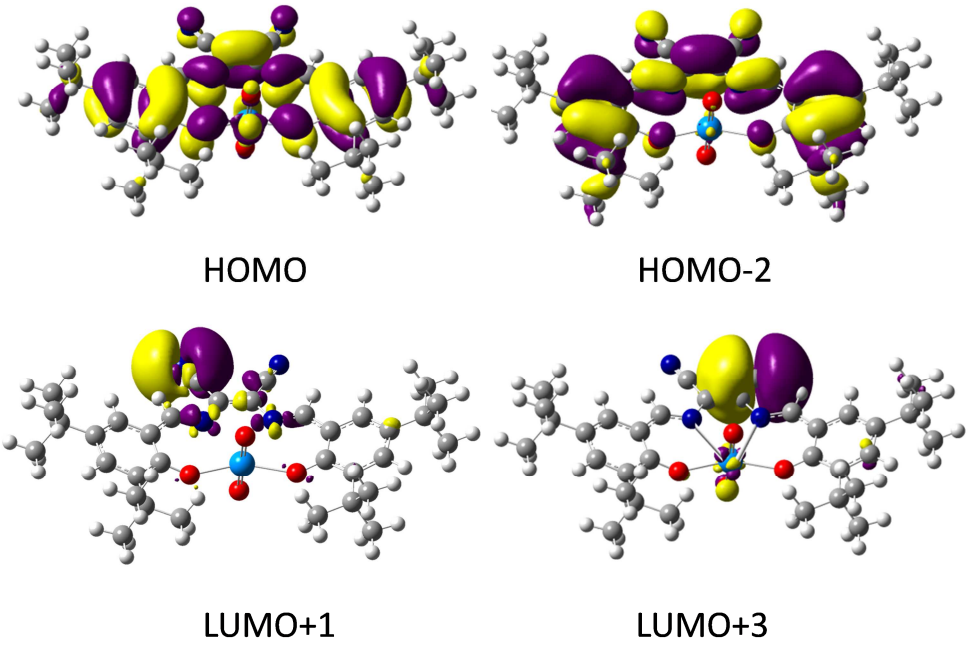

Figure 7

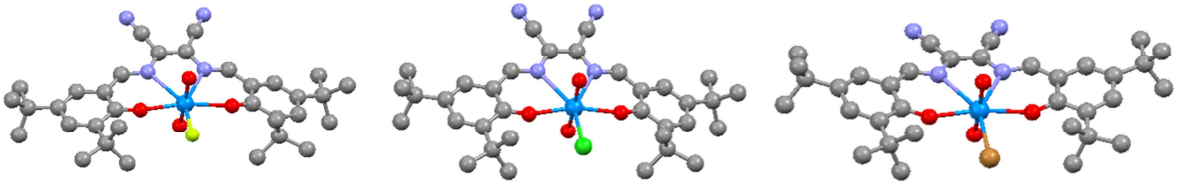

Figure 8

Tables

Table 1

	Halide	K (M^{-1})	
		1	**2**
$CHCl_3$	F^-	-[a]	$> 10^6$
	Cl^-	-[a]	$2 \cdot 10^5$
	Br^-	-[a]	$4 \cdot 10^3$
CH_2Cl_2	F^-	$> 10^6$	$> 10^6$
	Cl^-	$3 \cdot 10^5$	$5 \cdot 10^5$
	Br^-	$2 \cdot 10^4$	$1 \cdot 10^3$

Table 2

Complex	**Distance (Å)**		
	U=O	U-O	U-N
1	1.783	2.258	2.614
2	1.786	2.248	2.595

Table 3

	Vacuum	**CH_2Cl_2**	**$CHCl_3$**
1-F	-133.20	-67.54	-75.18
1-Cl	-61.94	-12.60	-18.31
1-Br	-47.81	-4.56	-8.88
2-F	-145.30	-87.50	-92.35
2-Cl	-72.53	-30.99	-34.38
2-Br	-56.55	-20.77	-23.68

Schemes

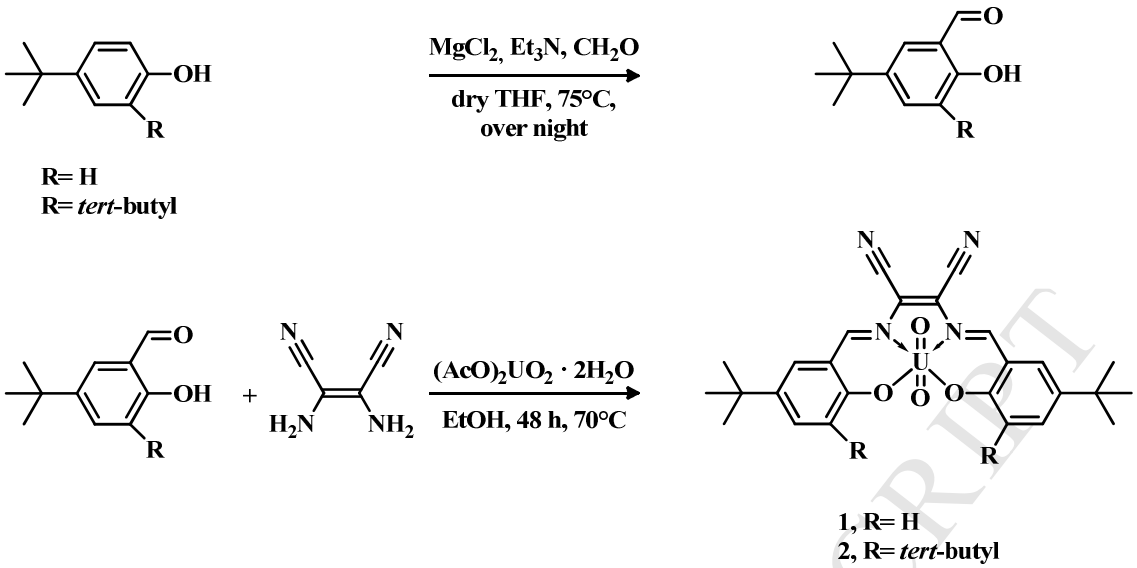

Scheme 1

Colorimetric and fluorescence "turn-on" recognition of fluoride by a maleonitrile-based Uranyl Salen-complex

Silvia Bartocci,[1] Ferran Sabaté,[2] Ramon Bosque,[2] Flore Keymeulen,[3] Kristin Bartik,[3] Laura Rodríguez,[2,*] Antonella Dalla Cort.[1,*]

[1] *Dipartimento di Chimica and IMC-CNR Sezione Meccanismi di Reazione, Università La Sapienza, Box 34 Roma 62, 00185 Roma, Italy. Fax: +39 06490421; Tel.: +39 0649913087.*

e-mail address: antonella.dallacort@uniroma1.it

[2] *Departament de Química Inorgànica, Universitat de Barcelona, Martí i Franquès 1-11, 08028 Barcelona, Spain. Fax: +34 934907725; Tel.: +34 934039130.*

e-mail: laura.rodriguez@qi.ub.es

[3] *Engineering of Molecular NanoSystems, Université libre de Bruxelles, 50 avenue F.D. Roosevelt, B-1050 Brussels, Belgium.*

Scheme's caption

Scheme 1. Synthetic route to Uranyl-salen complexes **1-2.**

Figures' captions

Figure 1. Compound **1** in $CHCl_3$ ($5 \cdot 10^{-5}$ M) and after addition of 1 equivalent of TBAF, TBACl, and TBABr.

Figure 2. Absorption spectra of **2**, $2.5 \cdot 10^{-5}$ M in $CHCl_3$ at 25°C upon addition of increasing amounts of TBAF (left). Inset: spectral changes of 2 with TBAF at 608 nm; Job Plot representation of the titration of **2** with TBAF (right).

Figure 3. Compound **2** in $CHCl_3$ ($5 \cdot 10^{-5}$ M) and after the addition of 1 equivalent of TBAF, TBACl, and TBABr

Figure 4. Emission spectra of complex **2** ($1.85 \cdot 10^{-5}$ M) in $CHCl_3$ for increasing additions of TBAF upto 30 equivalents.

Figure 5. Molecular modeling structure of **1** (left) and **2** (right). Carbon (grey); oxygen (red); uranium (pale blue); nitrogen (dark blue); hydrogens are omitted for clarity.

Figure 6. Molecular modeling structure of **1**-dimer (left) and **2**-dimer (right). Carbon (grey); oxygen (red); uranium (pale blue); nitrogen (dark blue); hydrogen (white)

Figure 7. HOMO and LUMO orbitals involved in the lowest energy transitions in **2**.

Figure 8. Molecular modeling structure of **2-F** (left), **2-Cl** (middle) and **2-Br** (right). Hydrogens are omitted for clarity. Carbon (grey); oxygen (red); uranium (pale blue); nitrogen (dark blue); fluoride (yellow); chloride (green) and bromide (brown).

Tables' captions

Table 1. Association Constants, K_a, between **1** and **2** and halide in $CHCl_3$ and in CH_2Cl_2 at 25°C.
[a]Not determined

Table 2. Main distances calculated for optimized geometries of complexes **1** and **2**.

Table 3. ΔE values (kcal/mol) calculated for the formation of **1** and **2**:halide adducts in vacuum both in CH_2Cl_2 and $CHCl_3$.

Colorimetric and fluorescence "turn-on" recognition of fluoride by a maleonitrile-based Uranyl Salen-complex

Silvia Bartocci,[1] Ferran Sabaté,[2] Ramon Bosque,[2] Flore Keymeulen[3], Kristin Bartik[3], Laura Rodríguez,[2,*] Antonella Dalla Cort.[1,*]

[1] *Dipartimento di Chimica and IMC-CNR Sezione Meccanismi di Reazione, Università La Sapienza, Box 34 Roma 62, 00185 Roma, Italy. Fax: +39 06490421; Tel.: +39 0649913087.*

e-mail address: antonella.dallacort@uniroma1.it

[2] *Departament de Química Inorgànica, Universitat de Barcelona, Martí i Franquès 1-11, 08028 Barcelona, Spain. Fax: +34 934907725; Tel.: +34 934039130.*

e-mail: laura.rodriguez@qi.ub.es

Highlights

- Two new uranyl-salen complexes based on a 1,2-diaminomaleonitrile are described.

- Spectroscopic studies proof their potential use for fluoride detection.

- The presence of two bulky substituents favors the molecular recognition process.

- DFT calculations support the experimental data.